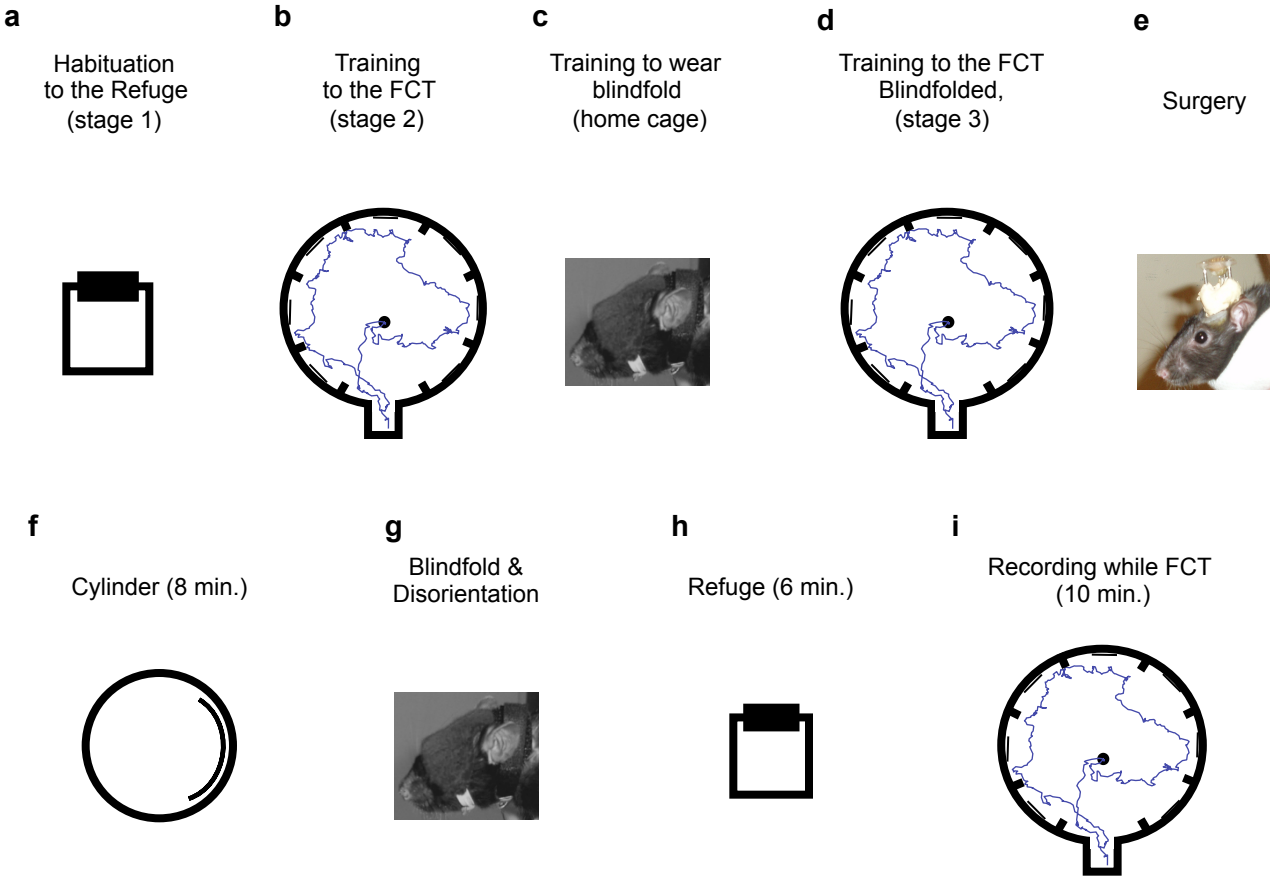

Supplementary Figure 1: Sequential order for behavioural training (a-d) and recording procedures (e-h). (a) The animals were habituated to eat in the refuge for 3 days. The door of the refuge was closed and they had 10 min to eat the 10 food pellets placed in the refuge (stage 1). (b) The animals were then trained to perform the food-carrying task (FCT). By the end of this second training stage, the animals were habituated to wear the blindfold (c): 20 min/day in their home cage for at least one week. Once they were able to complete at least four foraging trips in < 10 min, the animals were trained to perform the task with the blindfold (d) until they reached the same criterion (4 trips $\leq$ 10 min). (e) The animals were implanted with an array of recording electrodes in the anterodorsal thalamic nucleus (ADN). (f-i). Recording procedure: after recovery, the activity on each of the 10 electrode wires was monitored daily as the animal foraged for small food pellets thrown randomly inside a grey cylinder apparatus (diameter: 76 cm, height = 51 cm). The cylinder contained a large white cue card occupying ~100°of arc attached along the inside of the cylinder wall (f).

The apparatus was surrounded by floor-to ceiling black curtains arranged in a 2.5 m diameter circle. A white noise generator near the ceiling centre was used to mask extraneous sounds. When a HD cell was isolated, a baseline session was recorded in the cylinder for 8 min. Two light-emitting diodes (LEDs ~ 12 cm apart) positioned above the rats' head along its longitudinal axis were monitored (60 Hz) to indicate the rat's directional heading. (g) Then the animal was blindfolded and underwent a disorientation procedure. (h) The animal was then placed in the refuge area (29×30 cm), and the cell was recorded for 6 min with the door closed. (i) Then the door of the refuge was opened and the rat was allowed to forage for food pellets for 10 min. The pellet locations were varied pseudo-randomly and only one of the twelve cups was baited at a time. The cell's PFD was analysed off-line (LabView) for each excursion, which included both outbound and inbound trips, as well as for the inter-trial intervals (time spent in the refuge in between the two excursions). The outbound trip was defined as the animal's path from the refuge to the cup containing the food. The return trip was defined as the animal's path from the food cup to the wall of the apparatus, but not its path from the peripheral wall to the refuge.

Supplementary Figure 2: Photograph of recording site. (a) schematic diagram of a coronal slice at the level of the anterior thalamic nuclei: 1.40 mm posterior to bregma. (b) Photograph of a coronal slice stained with thionin, showing the electrode track (arrow) passing through the anterior dorsal thalamus (ADN). Dashed line indicates the boundaries of ADN.

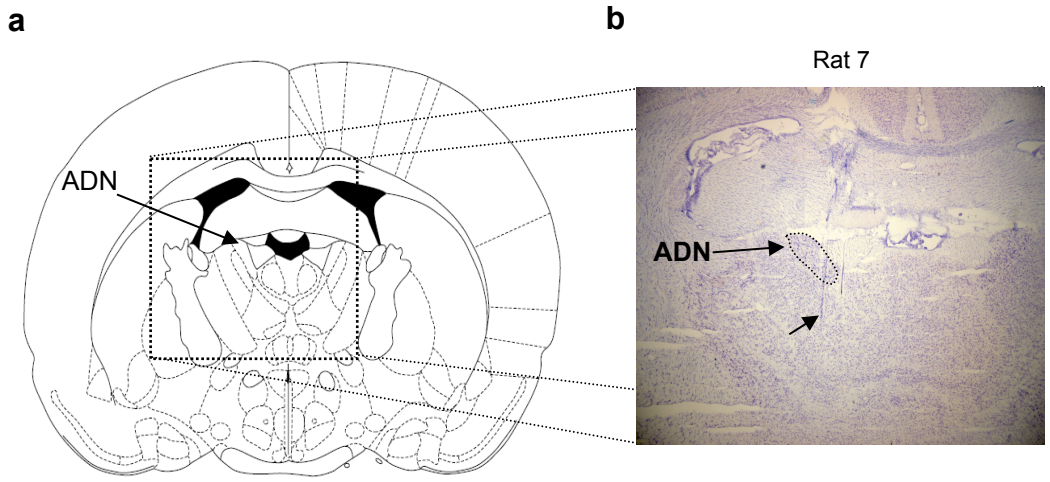

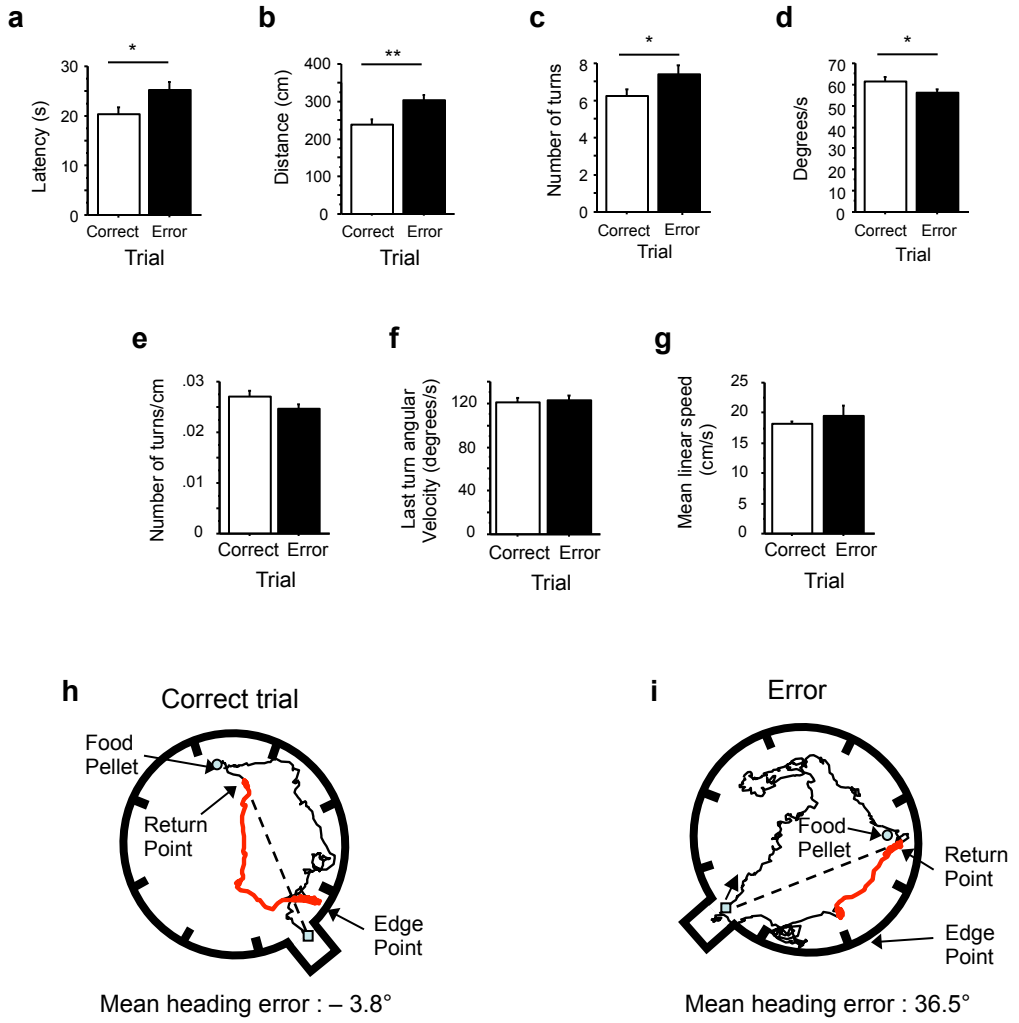

Supplementary Figure 3: Behavioural measures. Two LEDs permitted continuous tracking of the rats, which was used to perform the following off-line analyses: (1) the time spent foraging before finding the food, (2) the distance of the animal's path, (3) the rat's angular head velocity during the outbound trip (every 0.5 sec), (4) the number of head turns - a head turn was defined as head movements that reached at least an angular head velocity $\geq$ 80°/sec, and (5) the angular velocity in the last turn made by the animal after it found the food and initiated its return. Using these measures we computed (6) the linear speed and (7) the number of turns per cm. **a,** Average duration of the outward trips (correct *vs.* incorrect trials; * $P < 0.05$). **b,** Average distance covered in outward trips in correct *vs.* incorrect (error) trials (** $P < 0.01$). **c**, Average number of turns in outward trips (correct *vs.* incorrect trials; * $P < 0.05$). **d**, Mean angular velocity in outward trips (correct *vs.* incorrect trials). **e**, Mean number of turns per second recorded during the outbound trip in correct *vs*. error trials (P=0.09). **f**, Angular head velocity of the last turn in correct *vs*. error trials (P=0.60). **g**, Mean linear speed during the outbound trips in correct *vs*. error trials (P=0.46). **h-i**, Two representative trials. The trial starts when the rat initiates its outbound trip (indicated by a square). The location of the food pellet is indicated by a circle.

Once the rat has found the food, it initiates a homeward trip until it finds the refuge. The part of the homeward trip that has been used for behavioural analyses is shown in red and ends when the rat reaches the edge of the arena. If the animal reaches the edge of the arena between the two vertical barriers adjacent to the refuge, the trial is counted as correct (h). If the animal reaches the arena edge outside these two adjacent barriers, the trial is counted as an error (i). We calculated the mean heading of the animal in its homeward trip (return point to edge point) by measuring the animal's moment-to-moment HD from the time it was approximately one body length away from the place where it found the food pellet to the time when it reached the edge of the arena (see examples: Return point). The mean heading between these two points was then subtracted from the direction of the direct return to the refuge (dashed line) and this value was defined as the mean heading error. In some trials the rats returned to the refuge without having found the food pellet; these trials were included in the analyses when a clear return path was identified (n=64, see details and examples in Supplementary Figure 15).

Supplementary Figure 4: Behavioural characteristics of the outward trip and homing accuracy. Figures (**a-d**) plot the absolute heading errors the animals made in their homing trips, against respectively (**a**) the duration of the outward trip, (**b**) the distance of the outward trip, (**c**) the number of head turns during the outward trip, and (**d**) the mean angular velocity of these turns. In all of these cases, the linear correlations were weak (all r's < 0.2). Figures (**e-h**) plot the distributions of these four behavioural measures on correct (blue) and error (red) trials.

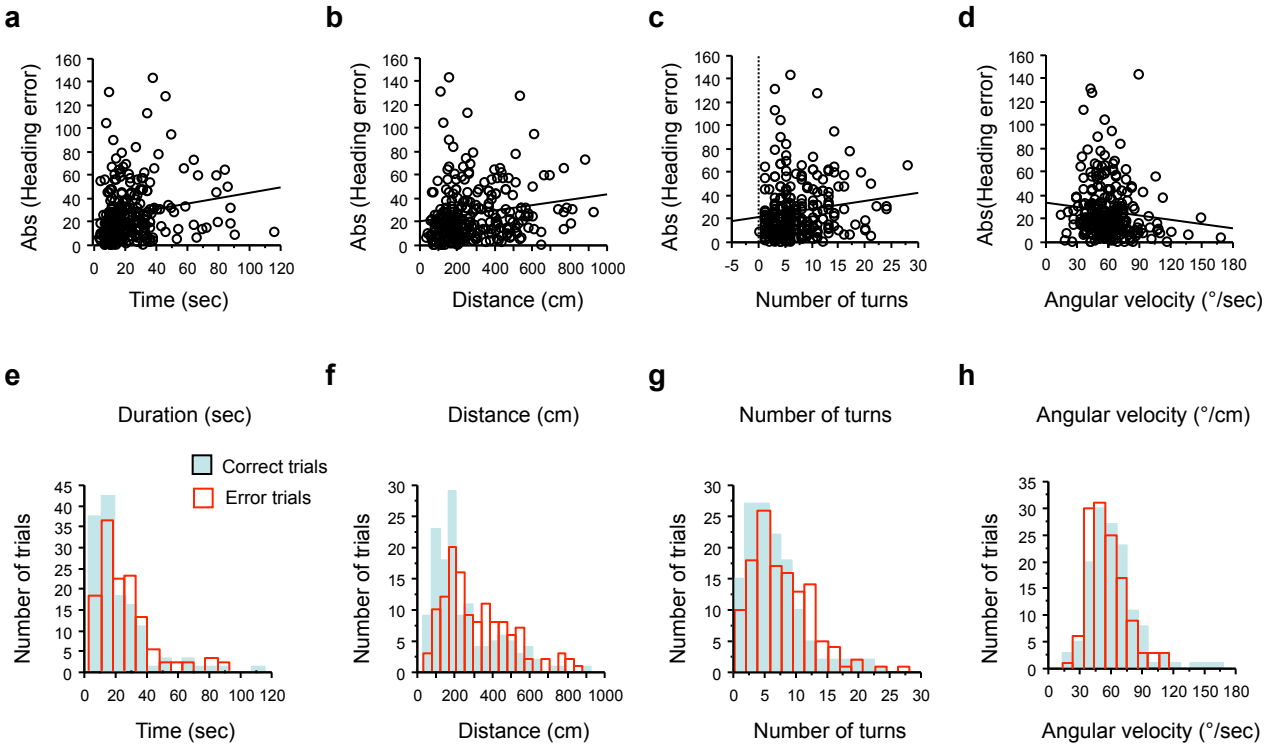

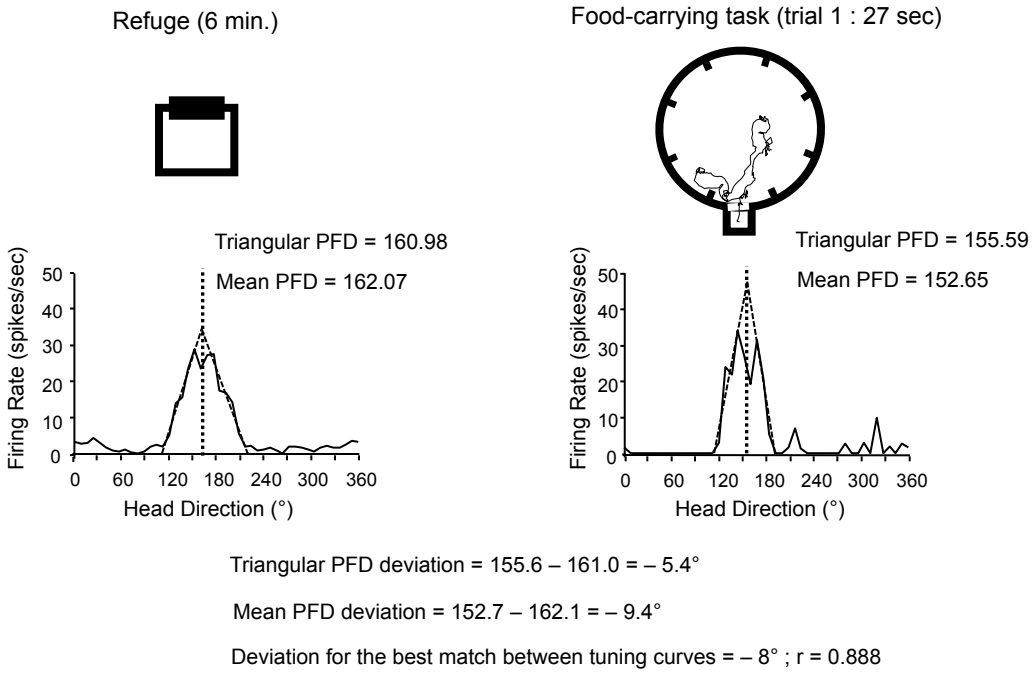

Supplementary Figure 5: The firing properties of the HD cell (peak firing rate, preferred firing direction, directional firing range) were determined by fitting a triangular model to the firing rate *vs*. HD graphs (see example below) (Taube et al., 1990). Three methods were used to quantify the amount of shift in the preferred firing direction (PFD) of a HD cell: (1) a simple subtraction of the two *triangular* PFDs measured (i.e., PFD during trial n – PFD in the refuge), (2) a subtraction of the *mean firing directions* recorded in each episode. The mean firing direction was calculated from the firing rate *vs*. HD tuning function by determining the centre of mass using ± 8 bins (64°) on either side of the bin with the maximal firing rate, (3) an algorithm that maximized the cross-correlation between the firing rate *vs*. HD functions for the two sessions or trials. The function of one episode was shifted in 8° increments relative to the function of the second episode. The angular shift that yielded the maximum cross-correlation (Pearson's *r*) was defined as the difference in PFD between trials. We chose to use the second method for all our quantitative analyses because it did not require the experimenter to define each leg of the triangle (a subjective process; first method) and was not limited to ± 8° bin values (third method). However, the two other methods yielded similar results. Some artefacts, caused by the rat's head bumping into the edge of the apparatus, occurred and were excluded from the analyses. As mentioned in the article, there was no difference between correct *vs*. error trials in the directionality of HD cells (Raleigh *r*). It follows that the circular standard deviation (SD = [2*(1-*r*)]½) also shows a similar result regarding the dispersion of firing in each trial: no difference was observed between correct (SD = 45.8°) and error trials (SD = 46.9°) (P>0.05). To verify that the shift in the PFD observed between the initial refuge session (~ 6 min duration) and the inter-trial interval (mean duration = 52.2 ± 2.0 sec) was not due to the difference in sampling time, we sub-sampled the refuge session (1 sample was taken out of 7) in order to match the inter-trial duration. No significant difference was observed between these two measures of the cell's PFD in the initial refuge session (mean difference of 2.95 ± 0.18°). On five occasions two HD cells were recorded simultaneously for 20 trials. To avoid unfairly weighting the results from these sessions, due to double values from these behavioural analyses, only one occurrence (the cell visible in the larger number of trials in the session) was included in the analyses (n = 263). However, the results from both cells were included in all the analyses concerning the PFD shifts, which explains the higher number of trials in Figure 3a (n = 283).

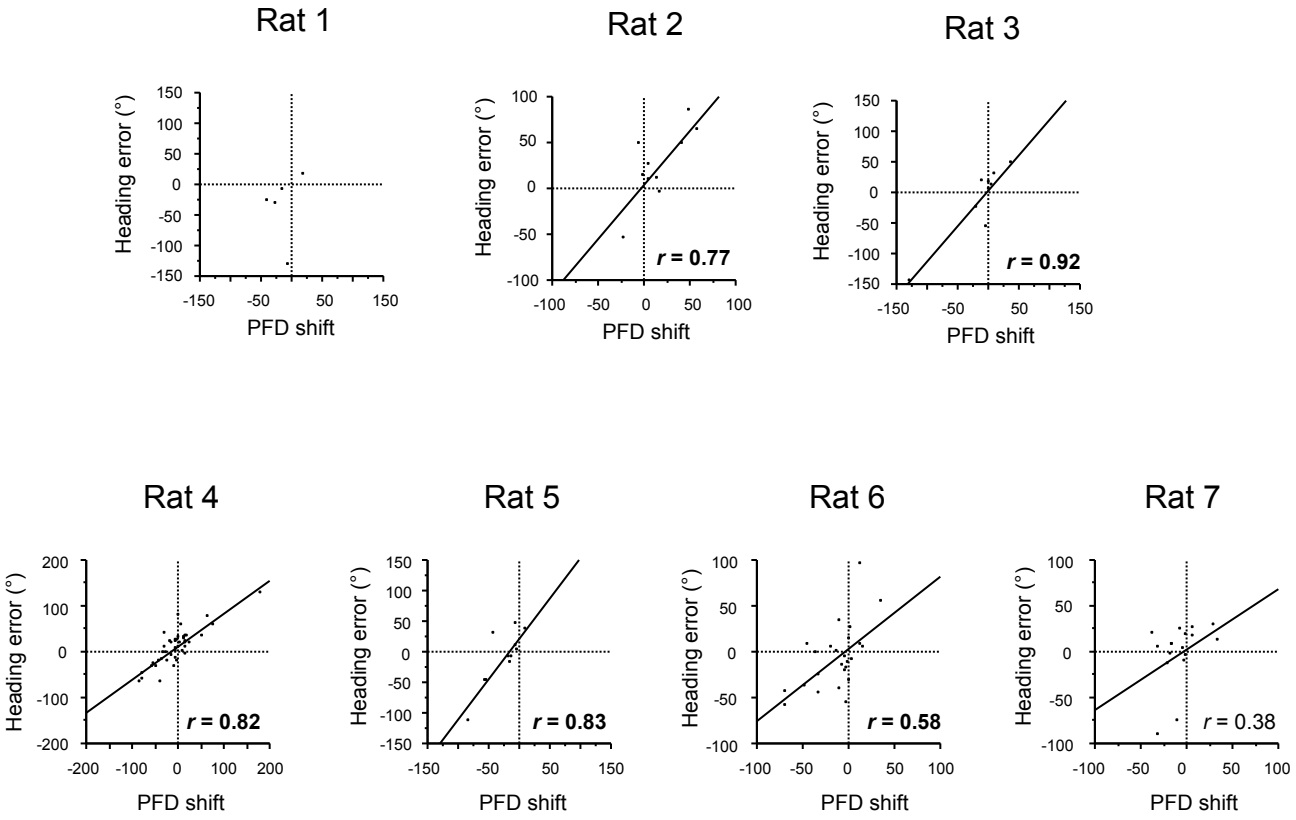

Supplementary Figure 6: Heading error as a function of the amount of shift in the PFD between the PFD in the refuge (during the inter-trial interval) and the PFD recorded in the following excursion. Because of the limited sampling conditions during inter-trial intervals only four values could be recorded for Rat 1, no correlation coefficient was calculated for this animal. For the other six animals, significant correlations (r) are indicated in bold ($P < 0.05$).

Supplementary Figure 7: Changes in the cell's PFD during the foraging trip. Five representative examples are shown. (a) Example of an outbound search path and an inbound return path. The return trip is shown in red. (b) Tuning curve (red) of a HD cell recorded during the foraging trip. The PFD we used was measured from the start of the outbound journey to the "edge point" (the moment the animal reaches the edge of the arena during the inbound return). The cell's tuning curve recorded during the outbound journey can be compared with the cell's tuning curve recorded during the preceding inter-trial interval (in black). (c) HD × Time × Firing rate. Each trip (outbound + inbound paths) was divided in two equal periods of time. The animal's path for each portion of the trip is depicted within the arena (part 1 in green, part 2 in blue). Underneath each of these figures, the corresponding tuning curve for that portion of the trial is shown in similar colours and can be compared to the cell's tuning curve for the preceding inter-trial interval (black).

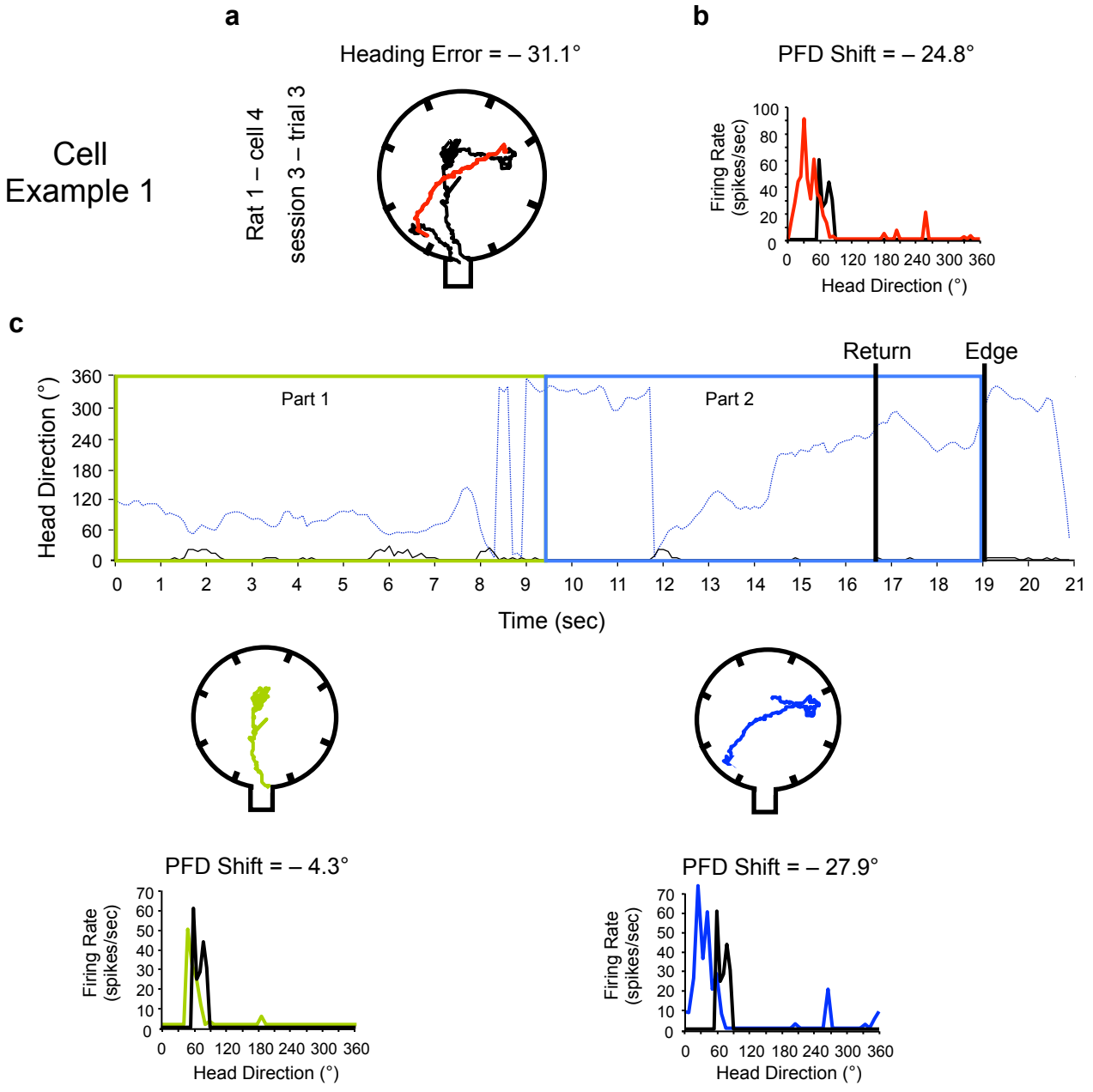

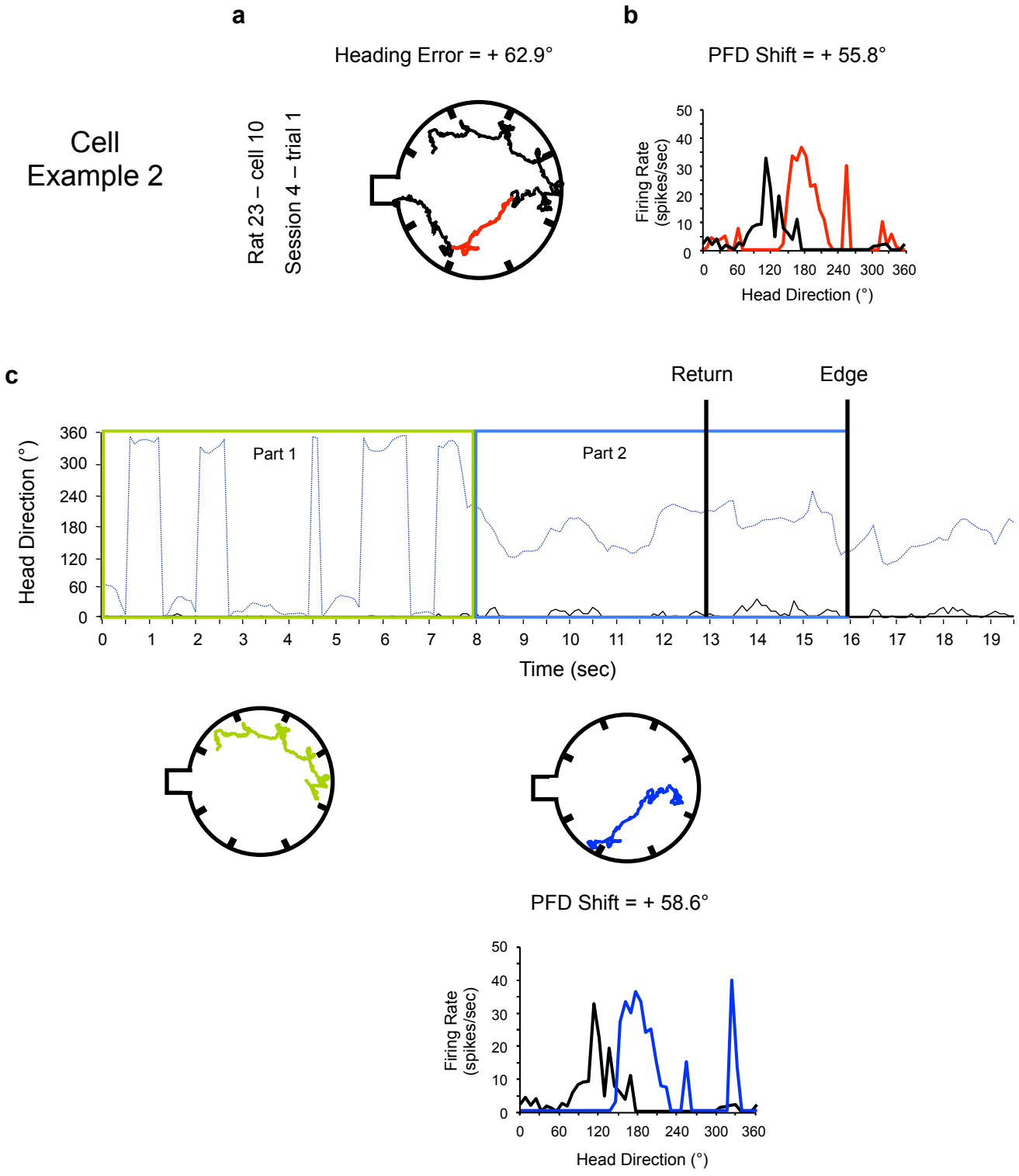

Remark: In this example, the firing of HD cell was not visible during the first part of the foraging trip, because the animal did not sample the direction of the cell's PFD. Therefore, the cell's PFD was obtained from the second part of the trip.

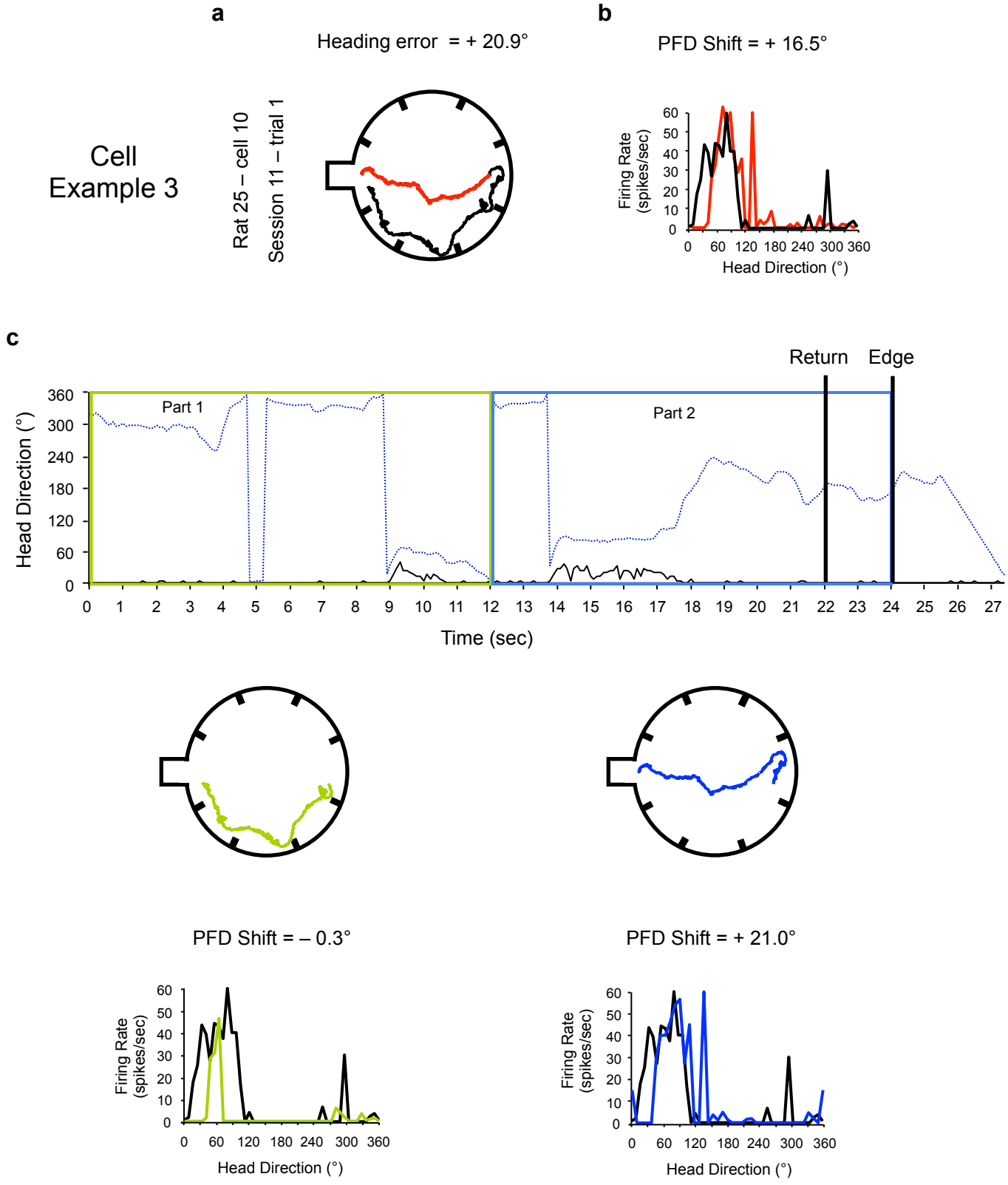
a
Heading error = + 20.9°
Cell
Example 3
Rat 25 – cell 10
Session 11 – trial 1
b
PFD Shift = + 16.5°
Firing Rate
(spikes/sec)
Head Direction (°)
c
Return
Edge
Part 1
Part 2
Head Direction (°)
Time (sec)
PFD Shift = – 0.3°
PFD Shift = + 21.0°

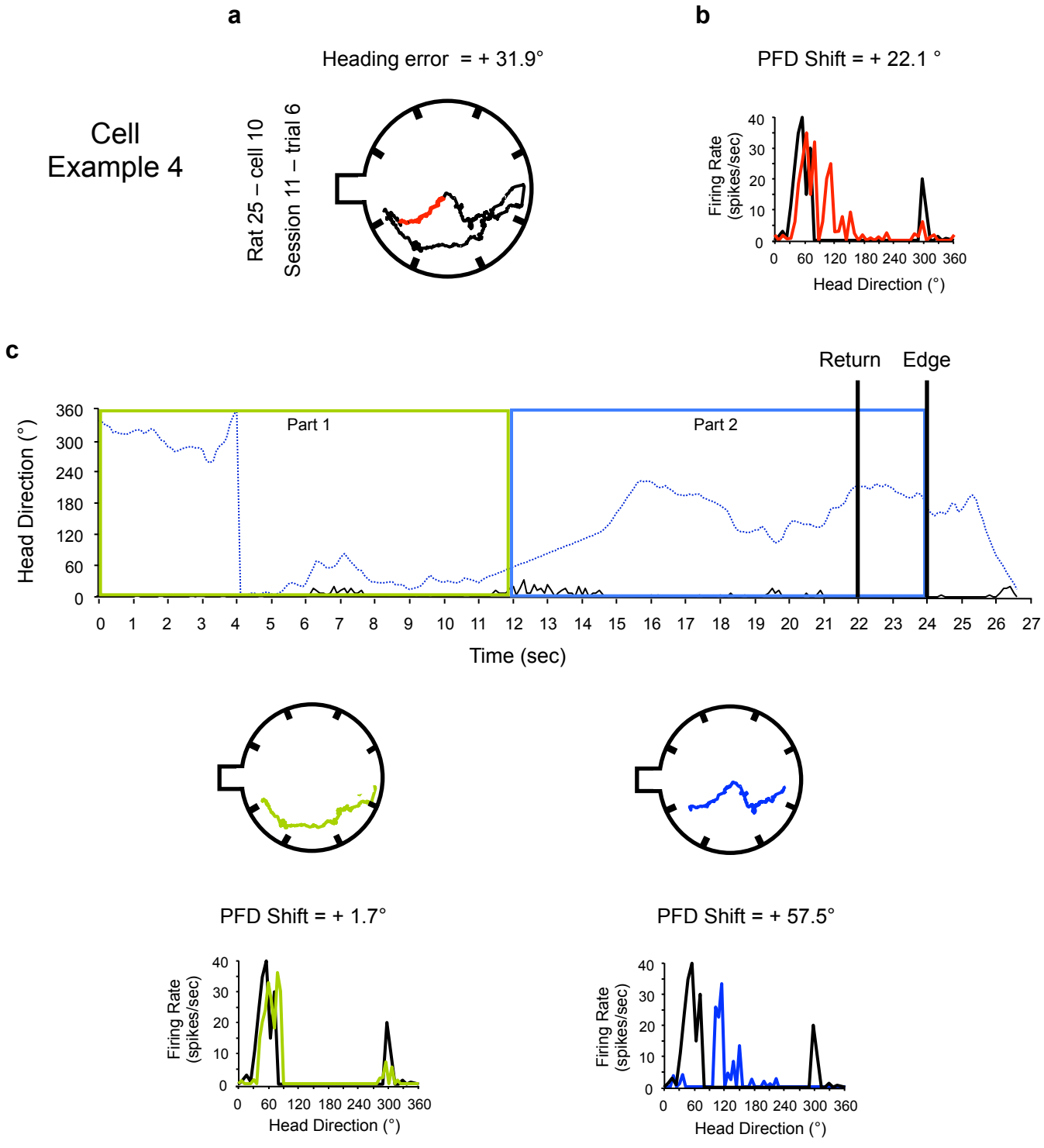
a
b
Heading error = + 31.9°
PFD Shift = + 22.1 °
Cell
Example 4
Rat 25 – cell 10
Session 11 – trial 6
Firing Rate
(spikes/sec)
Head Direction (°)
c
Return
Edge
Part 1
Part 2
Head Direction (°)
Time (sec)
PFD Shift = + 1.7°
PFD Shift = + 57.5°

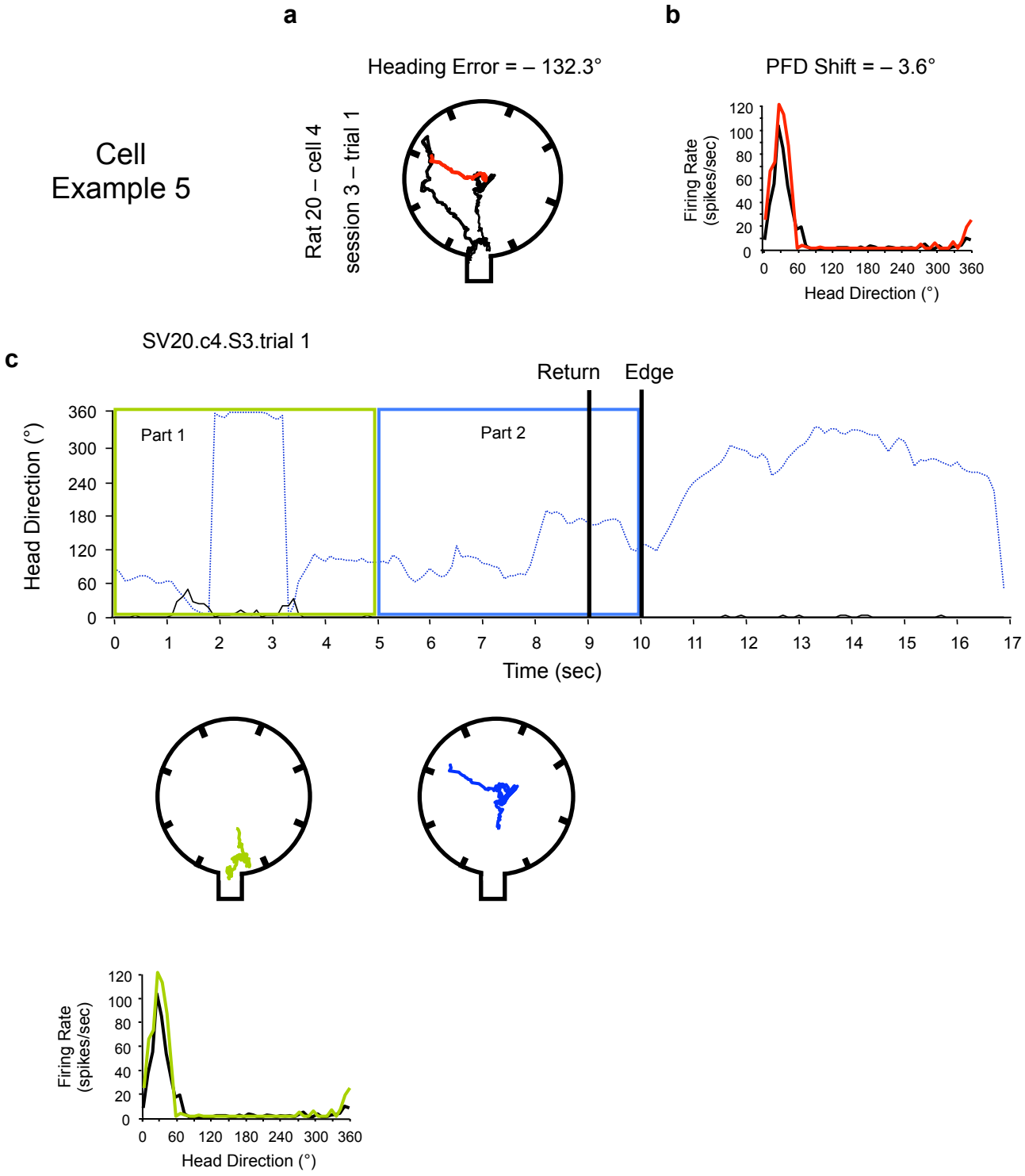

Remark: This example illustrates the alternative situation to the first example. In this case the cell's firing was not visible during the second part of the foraging trip because the animal did not sample the direction of the cell's PFD. Thus, the cell's PFD could only be measured from the first part of the trip, and gives a poor prediction of the animal's heading error.

Supplementary Figure 8: Changes in the cell's PFD during the foraging trip. Each foraging trip was divided in two equal periods of time, to determine whether the second part of the trip, which contains the return path, would give a better prediction of the animals' heading errors (see examples in Supp. Fig. 14). Indeed, in all the measures presented previously, we calculated the PFD shift using the cell's tuning curve averaged over the entire foraging trip (from the refuge start to the apparatus's edge on the return trip). However, the status of the HD system at the moment the animal initiates its return should be more accurate than the PFD recorded at the start of the excursion at the refuge. (a, b) Comparison of the prediction accuracy between heading error and PFD shift using the cell's PFD recorded in the first or second part of the foraging trip. (a) Direct comparison (ANOVA with repeated measures) of the first and second halves of the same trip ($P < 0.05$; $n = 48$). (b) Similar comparison, but including all values from both parts of the trip ($P < 0.05$; part 1 $n = 79$, part 2 $n = 89$).

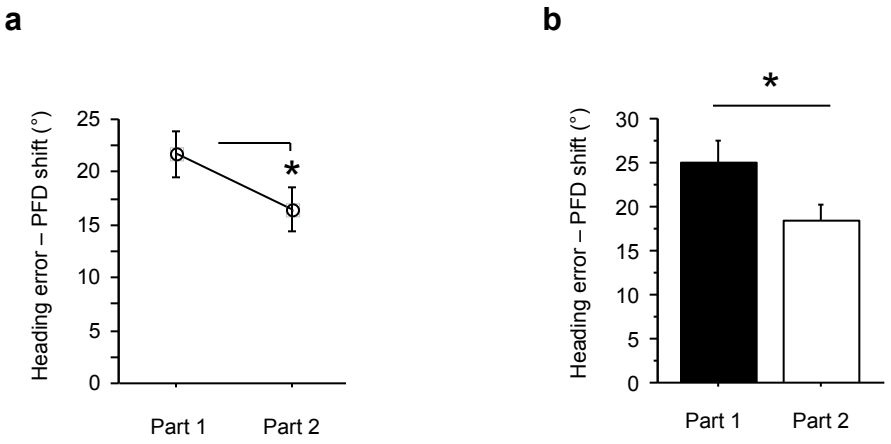

Supplementary Figure 9: Moment-to-moment changes in the cell PFD. Five examples are shown, with the left panels displaying the tuning curve of the cell recorded during a foraging trip, and the right panels displaying the moment-to-moment HD of the animal coupled with the cell activity (Firing rate × HD × Time). The red dots indicate the HD and time at which the cell's firing rate reached 50% of its maximum firing rate. The issue addressed here was to determine whether the PFD shifted gradually from the refuge value to the shifted value, or if the PFD 'jumped' to a new a value in a one-time shift phenomenon. In the few examples depicted here the cell's PFD can be monitored several times while the animal is foraging. Although a quantitative analysis is not possible with such a small number of trials, qualitatively, these examples support the view that the PFD shift occurs gradually throughout the trial, as the cell's PFD appears to drift from the refuge value to the new shifted value continuously while the animal forages in the apparatus. The refuge PFD value is indicated by the black line and the average PFD recorded during the foraging trip and used in our analyses is indicated by the red line. The respective tuning curves in the left panels are indicated using the same colours.

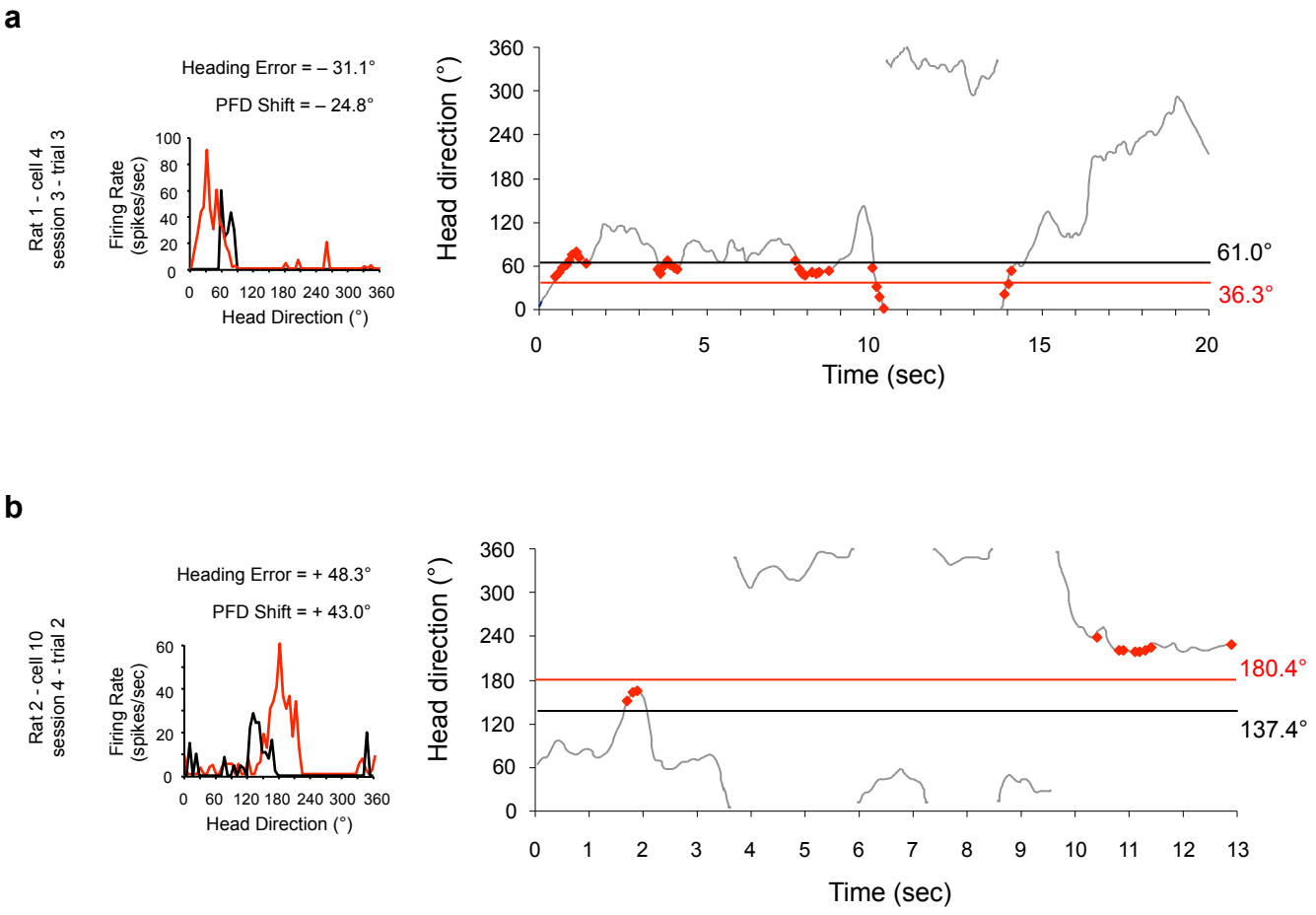

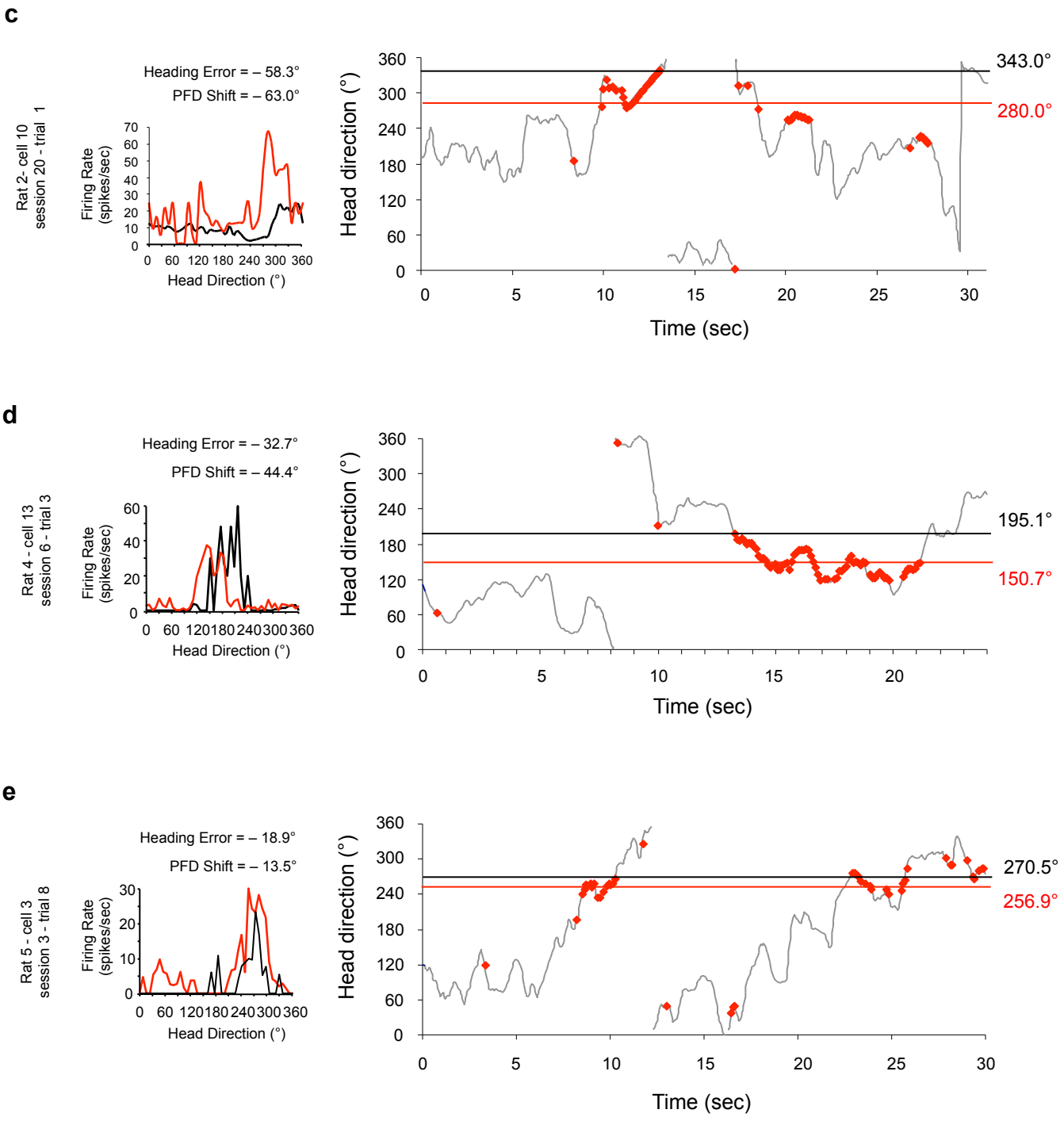

Remark: A previous study (Zugaro et al. 2003) showed that upon realizing that a visual cue had been rotated, the HD network can remap in less than 80 ms. We are not claiming that these shifts do not occur in this task, but it is interesting to note that even in remapping trials (examples b & c are remapping trials), the cell's PFD appears to drift gradually from its refuge value to the foraging trip value.

Zugaro MB, Arleo A, Berthoz A, Wiener SI. Rapid spatial reorientation and head direction cells. *J Neurosci* **23**, 3478-3482 (2003).

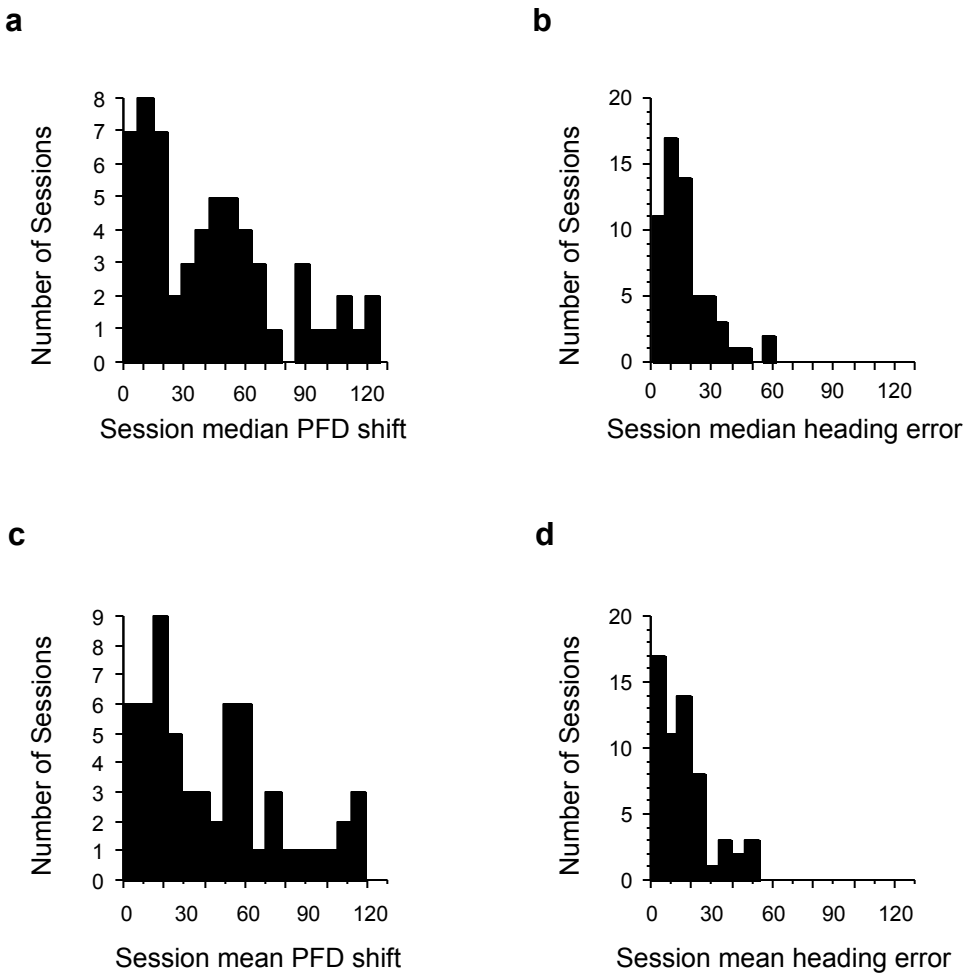

Supplementary Figure 10: Comparison between the distributions of (a) the session median PFD shift (also shown in Fig. 3f) and (c) the session mean PFD shift. Interestingly, these two distributions show comparable bimodal distributions, with a first mode around 0°, and a second mode around 50°. Such a bimodal distribution is not observed in the distribution of the session median heading error (b) (also shown in Fig. 3g), nor in the distribution of the session mean heading error (d), which are both clustered around 0°.

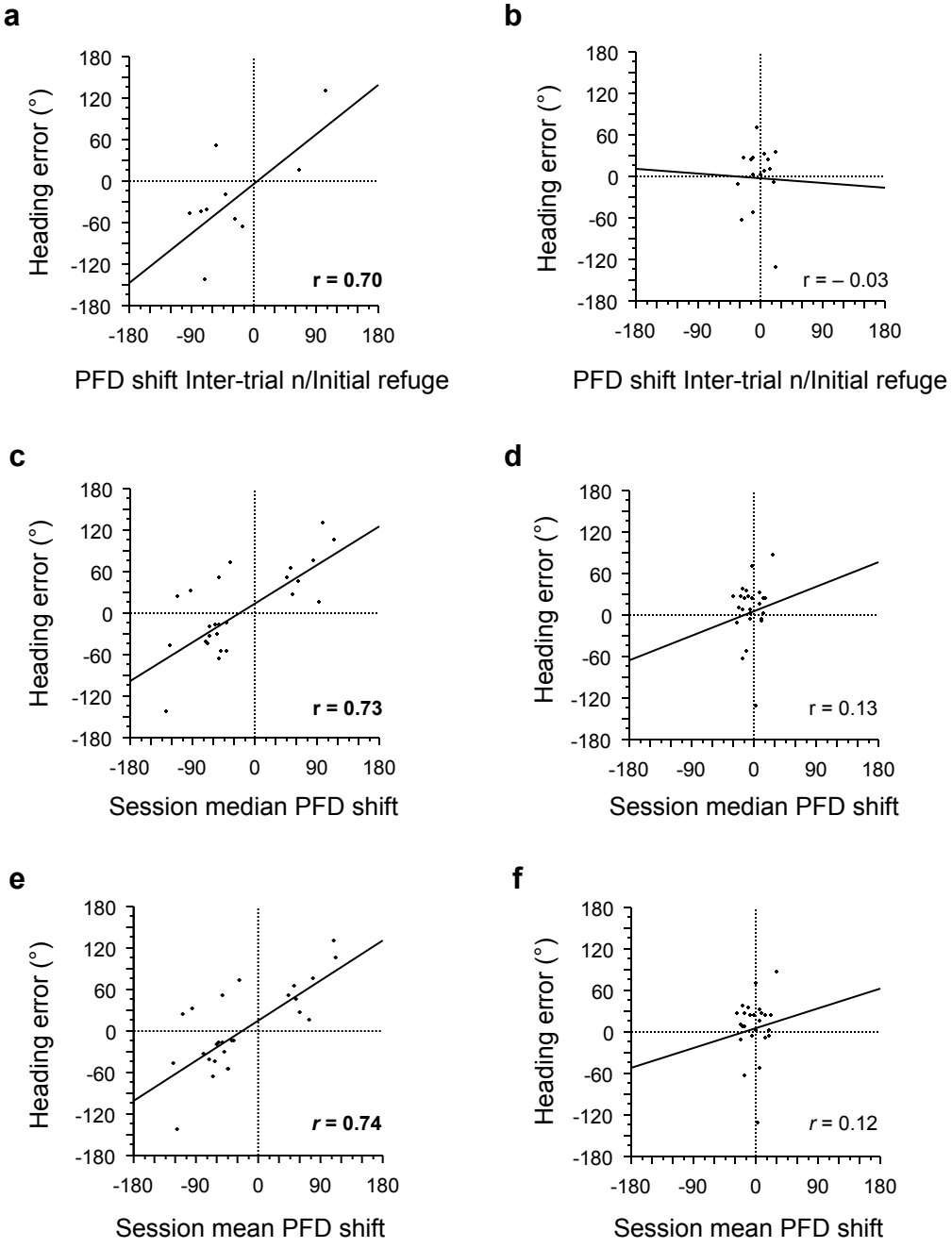

Supplementary Figure 11: The correction process. (a) Heading error as a function of the shift in the cell's PFD between the current inter-trial interval and the initial refuge (Mode 2 inter-trial intervals, also shown in the main manuscript, Fig. 5a). (b) For comparison, this graph shows the same analysis as in (a), but for Mode 1 inter-trial intervals. (c) Heading error observed in remapping trials, as a function of session median PFD shift compared to its initial refuge value (also shown in Fig. 5b). (d) For comparison, the same analysis as conducted in (c) is shown for resetting trials. (e) Heading error observed in remapping trials, as a function of session mean PFD shift compared to its initial refuge value. Note that using the session mean shift, instead of the session median shift, gives very similar results. (f) The same analysis as conducted in (e) is shown for resetting trials. Significant correlations (r) are indicated in bold ($P < 0.05$).

Supplementary Figure 12: Examples of remapping sessions. (a) After a heading error of 144.45° in the first foraging trip, the cell does not revert back to its initial refuge value (grey) upon return to the refuge (inter-trial 1, compare black to grey). The new (remapped) refuge value appears to be used as a new reference for the following trial, and the cell is reset to this remapped value in the following refuge periods (inter-trial 2). For this example, trial 1 is the remapping trial. (b) In this example the remapping trial is also trial 1, but in (c), remapping occurs in trial 2.

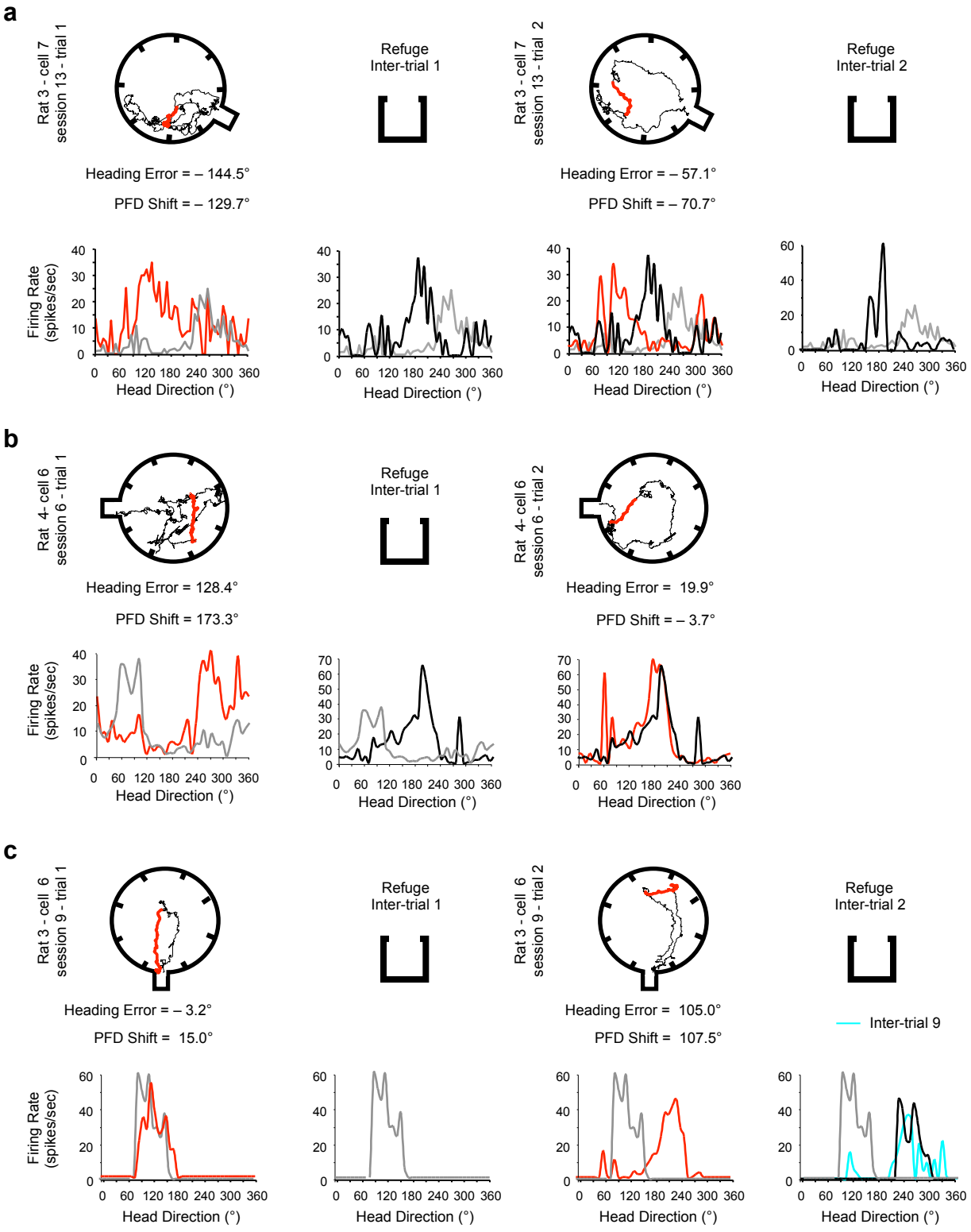

Supplementary Figure 13: Examples of resetting sessions. In these three examples (a-c), the foraging path of the animal is shown in the first row, with the outbound trip in black and the return trip in red. The tuning curve of the HD cell recorded at the corresponding time is shown below. The cell's tuning curve recorded in the initial refuge session is shown in grey, and can be compared with the tuning curves of the cell recorded during each foraging trip (red) and for the successive inter-trial intervals (black).

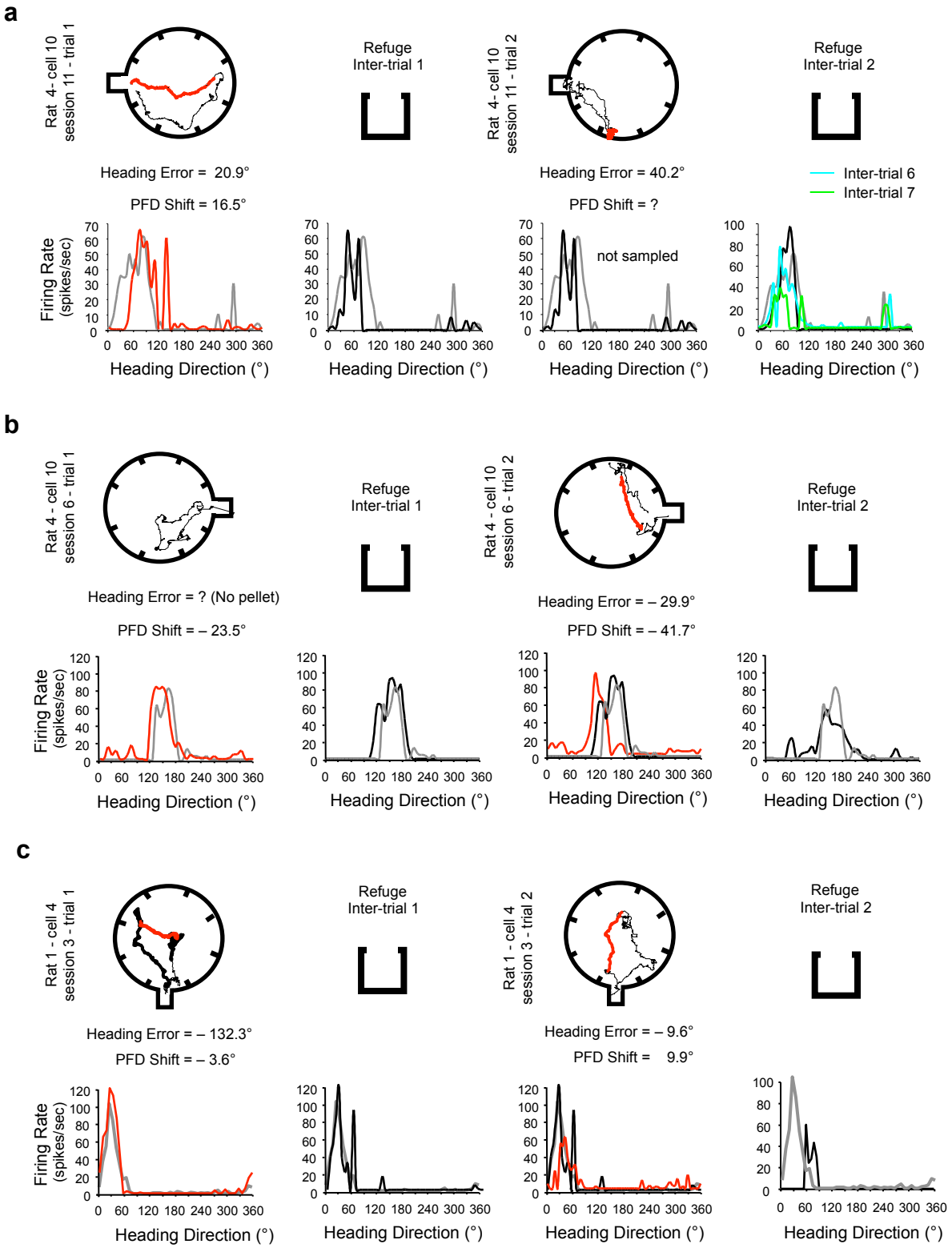

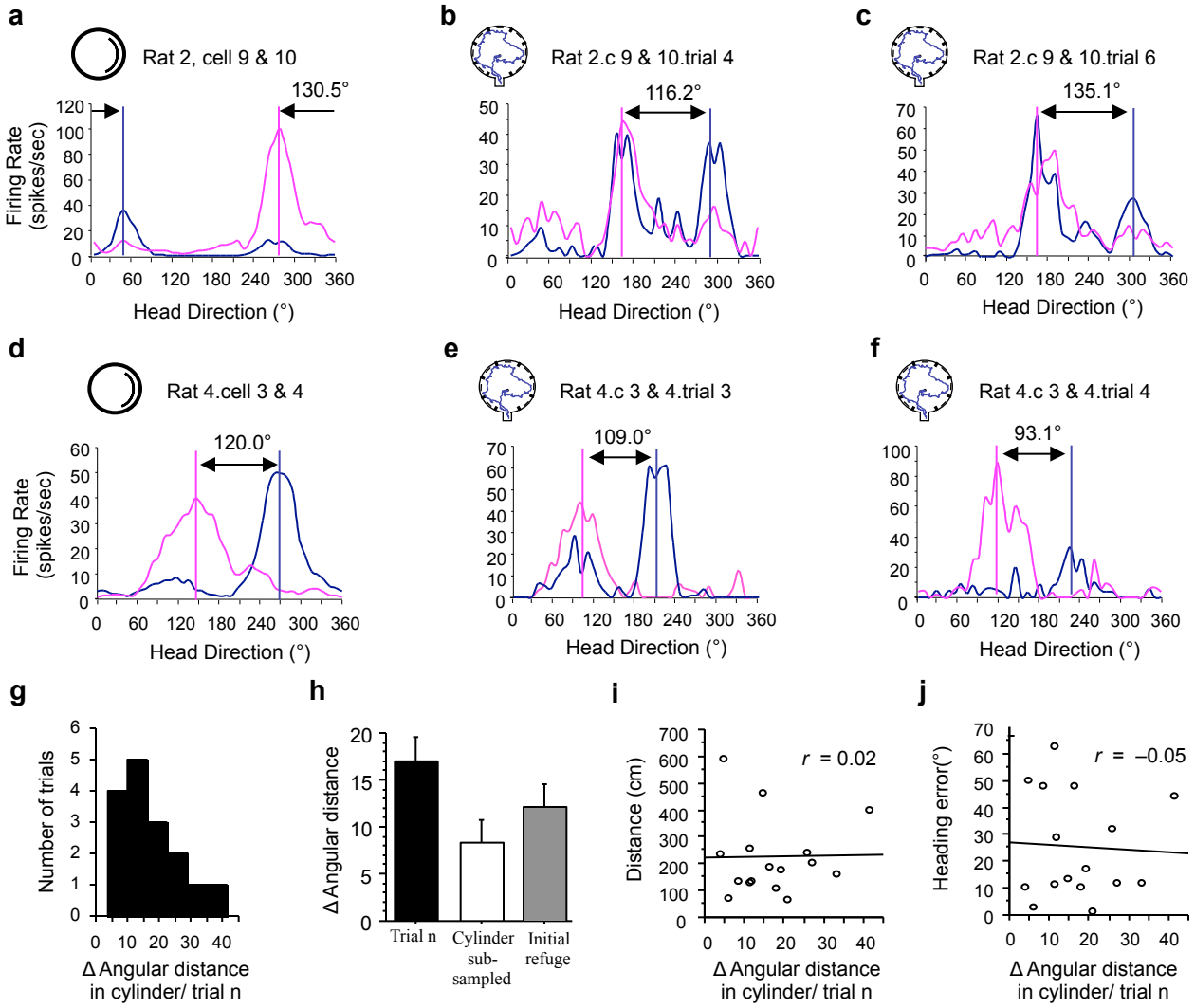

Supplementary Figure 14: Simultaneous recording of two HD cells. On five occasions (5 sessions, 20 trials), two HD cells were recorded simultaneously during the task. (a-f) Figures show representative examples of these sessions. In a and d we show the tuning curves of the cells recorded in the cylinder (8 min). For comparison Figures b, c, e, and f show the same cells recorded during the food-hoarding trials. On each graph we show the angular distance (AD) between the cells' PFDs. As observed in previous studies, the cells appear to move in register: see Figures a *vs.* b & c, both cells rotated -100° between the cylinder (a) and the food-hoarding apparatus (b & c). However, we also observed some variations in the AD of simultaneously recorded cells (see Figures d and f). Figure g shows the distribution of the differences between the AD in each trial and the AD in the cylinder. Several differences between the recordings conditions (cylinder *vs.* behavioural task) may explain these variations: (i) the behaviour, (ii) the sampling time (8 min in the cylinder *vs.* 24.31 sec on average for a foraging trip), (iii) the fact that the animals were blindfolded when performing the task, but not during the cylinder session. The average difference (AD in trial n – AD in cylinder) is shown in Figure h (black bar) and compared to variations observed when sub-sampling the cylinder session (AD in cylinder sub-sampled – AD in cylinder; white bar). The analysis revealed a significant difference, suggesting that sampling itself can not explain the variations observed ($P < 0.05$). However, the analysis also showed no difference with the variations observed in the refuge (when the animals are blindfolded, grey bar, $P > 0.05$), suggesting that the deprivation of visual cues may explain the AD variations of simultaneously recorded HD cells. Figures i & j show that the AD variations are not correlated with the distance covered by the animals (j) or with the heading error they made when homing (j).

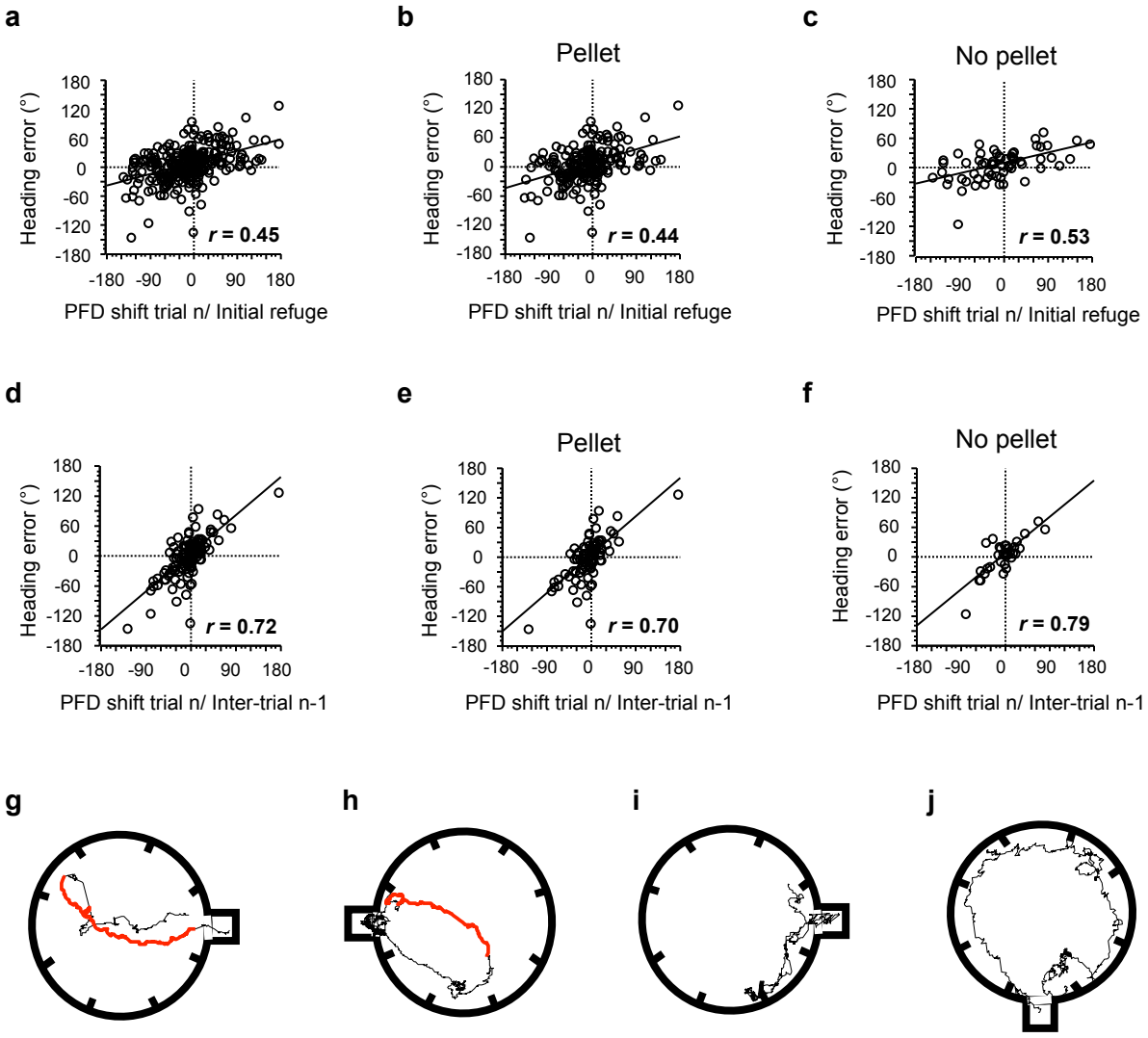

Supplementary Figure 15: "No pellet trials". (a) Heading error the animal made in its homing trip, against the PFD shift from the initial refuge value (also shown in the main text as Fig. 2f). (b, c) Plots showing separate analyses for trials in which the animals found the pellet and brought it back (b) (n = 199), and trials when the animals returned to the refuge before finding the food pellet (c) (n = 64). (d) Heading error plotted against the PFD shift observed in trial n compared to the previous inter-trial value (inter-trial n-1, also shown in the main text as Fig. 2i). (e, f) Plots showing separate analyses for Pellet trials *vs.* No pellet trials. (g-j) Figures showing representative examples of No pellet trials. On g and h distinct return paths could be identified: after a stop the animals showed clear homing behaviour. Off-line behavioural analyses (blind to the fact that the animal found the pellet or not) were done to assess whether or not a return point could be determined. When possible, the trial was included in the analysis. Figures a-f demonstrate that the results are very similar with or without these "No pellet" trials. Figures i and j show representative examples of trials that were excluded from our analyses: these trials were more explorations of the apparatus (most of the time along the wall) than foraging trips. In these cases, both the return point, and the edge point were impossible to determine. Significant correlations (r) are indicated in bold ($P < 0.05$).

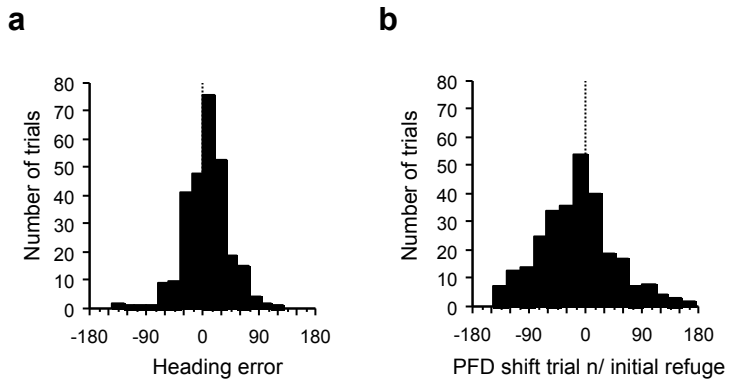

Supplementary Figure 16: Distribution of the angular values used in the correlation analysis shown in Figure 2f. (**a**) Distribution of the heading errors of the animals. In most trials the rat's heading error was < 90°. On eight occasions the heading error was > 90°. This distribution was mostly restricted to a half-circle (–90°/+90°), which implies that linear statistical analyses can be used for these data (Batschelet, 1981, pg. 231). (**b**) Distribution of the PFD shifts (PFD trial n – PFD initial refuge) reveals a wider distribution. In a few cases, the PFD shift is > 150° (5 occasions), which for correlation analyses could result in lowering the r value because of the 0-360° boundary problem (here +180°/–180°: the heading error could be on one side (+170°), and the PFD shift on the other side (–170°), which would result in creating an artificial outlier because of the circular nature of the data. However, because of the limited range of heading errors we observed (a), this problem was not an issue and linear statistics could be used to analyse our data set.